

Scheelite to fergusonite phase transition in YLiF_4 at high pressuresA. Grzechnik,^{1,*} K. Syassen,¹ I. Loa,¹ M. Hanfland,² and J. Y. Gesland³¹Max-Planck-Institut für Festkörperforschung, Heisenbergstrasse 1, D-70569 Stuttgart, Germany²European Synchrotron Radiation Facility, BP 220, F-38043 Grenoble, France³Université du Maine Cristallogénèse, F-72085 Le Mans, Cedex 9, France

(Received 2 October 2001; published 7 February 2002)

Yttrium lithium orthofluoride YLiF_4 with a tetragonal scheelite structure ($I4_1/a$, $Z=4$) has been studied with angle-dispersive x-ray powder diffraction in a diamond anvil cell at room temperature. Upon compression to about 10.0 GPa, the c/a axial ratio increases, demonstrating that the tetragonal distortion of the fluorite superstructure is enhanced. At 10.6 GPa, there occurs a transformation to a fergusonite structure ($I2/a$, $Z=4$) that involves small distortions of the cation matrix and significant displacements of anions in the simple cubic packing. There is no detectable discontinuity in the evolution of the unit cell volumes during the $I4_1/a \rightarrow I2/a$ transformation. Changes of the lattice parameters and axial ratios are similar to those found for temperature-induced ferroelastic scheelite-fergusonite transitions in rare earth orthoniobates and orthotantalates. A second sluggish phase transition to an as yet unidentified polymorph of YLiF_4 occurs above 17.0 GPa.

DOI: 10.1103/PhysRevB.65.104102

PACS number(s): 61.50.Ks, 62.50.+p, 77.80.Bh

I. INTRODUCTION

Yttrium lithium tetrafluoride is a commercially used host material for solid state lasers. YLiF_4 , isomorphous with LnLiF_4 ($\text{Ln}=\text{Eu}-\text{Lu}$), has a scheelite (CaWO_4 -type) structure ($I4_1/a$, $Z=4$) which is a superstructure of fluorite CaF_2 ($Fm\bar{3}m$, $Z=2$).^{1,2} The fluorine atoms are in a distorted simple cubic arrangement and the Y^{3+} and Li^{1+} cations are eightfold and fourfold coordinated by fluorine, respectively (Fig. 1). Such rare earth complex fluorides of lithium are not formed for the light rare earth $\text{Ln} = \text{La} - \text{Sm}$ series.¹ However, the Y^{3+} ions in YLiF_4 can be replaced by light trivalent lanthanide ions, so that related optical transitions between crystal field levels of the lanthanide ions lead to luminescence properties of technological importance.

YLiF_4 has been extensively studied at various temperature conditions to better understand the chemical bonding and the interactions between central cations and their crystalline environment.³ Concerning the structural behavior at high pressures, Raman scattering measurements at room temperature indicate a structural phase transition at about 7 GPa.⁴ Luminescence experiments on $\text{YLiF}_4:\text{Eu}$ at $T = 300$ K do not show any anomaly at 7 GPa but evidence a reversible transformation in the pressure range from 10.0 to 10.5 GPa, associated with a lowering of crystal symmetry.⁵ Low-temperature luminescence measurements of Nd-doped YLiF_4 indicate a very subtle anomaly in the structural parameters of the scheelite phase near 6 GPa, and again very clearly a structural transition near 10.3 GPa.⁶

In this study we are interested in the structural properties of YLiF_4 at high pressures. We have studied its structural properties at room temperature using synchrotron angle-dispersive x-ray powder diffraction in a diamond anvil cell. Our x-ray powder diffraction data provide information on structural details of the scheelite phase that could be used as input for crystal field level calculations of rare earth doped materials as a function of hydrostatic pressure. Our main focus is on the pressure-induced structural phase transfor-

mations in this compound. We have identified the high-pressure phase present above 10 GPa as being of the fergusonite type. To the best of our knowledge, the new high-pressure polymorph of YLiF_4 is the first reported fergusonite phase in orthofluorides. The details of the scheelite-fergusonite phase transition resemble those of corresponding temperature-driven ferroelastic phase transitions in rare earth orthoniobates and orthotantalates. We have observed a second phase transition of YLiF_4 near 17 GPa and discuss possible structure candidates for this phase.

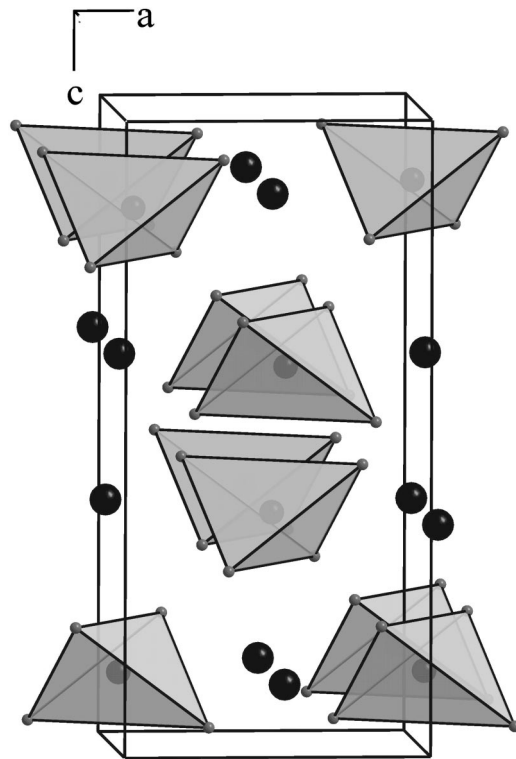


FIG. 1. Crystal structure of YLiF_4 at ambient conditions ($I4_1/a$, $Z=4$). The Li atoms are tetrahedrally coordinated. Large black solid symbols are Y atoms.

II. EXPERIMENTAL

The YLiF_4 crystals used in this study were doped with 2% Nd. It is the same material used for the luminescence studies in Ref. 6. A single crystal was ground to a fine powder and loaded into a diamond anvil cell with a methanol-ethanol pressure medium. We chose this medium to ensure a full comparison of the present x-ray diffraction results with the ones of the previous room-temperature Raman scattering⁴ and luminescence⁵ studies. Angle-dispersive powder x-ray diffraction patterns were measured at the ID9 beamline at the European Synchrotron Radiation Facility, Grenoble. Monochromatic radiation at a wavelength of 0.4203 \AA was used for pattern collection on image plates. The images were integrated using the program FIT2D (Ref. 7) to yield intensity versus 2θ diagrams. The instrumental resolution, i.e., the minimum full width at half maximum (FWHM) of diffraction peaks was 0.04° . To improve powder averaging, the DAC was rotated by $\pm 3^\circ$. The ruby luminescence method⁸ was used for pressure measurement.

Full Rietveld refinements of the x-ray diagrams were carried out using the program GSAS.⁹ The refined parameters were cell parameters, the fractional coordinates, isotropic thermal parameters, a Chebyshev polynomial background, Stephens profile function parameters,¹⁰ and an overall intensity scaling factor. A preferred orientation correction was not considered. The Stephens function was used in this work because it incorporates broadening of reflections due to strain, stacking faults, and shear stress that could develop under not fully hydrostatic conditions. Hence, systematic errors in Rietveld refinements due to the nonhydrostatic effects are minimized.

III. RESULTS

Diffraction diagrams of YLiF_4 measured at different pressures at $T=300 \text{ K}$ are shown in Fig. 2. At pressures up to about 10.5 GPa, all diffraction peaks are due to the scheelite structure ($I4_1/a$, $Z=4$). At higher pressures, a peak splitting and appearance of additional weak reflections indicate a phase transition to a polymorph with a structure that appears to be a distortion of the low pressure one. This first high-pressure phase sluggishly transforms to another polymorph starting at about 17.0 GPa and with a broad pressure range at which the first and second high-pressure phase coexist. Upon decompression from 24.8 GPa, diffraction patterns characteristic of the second phase are observed down to about 10 GPa. The scheelite phase is obtained again upon fully releasing the pressure.

Selected patterns of the scheelite polymorph^{1,2} were refined with the Rietveld method⁹ to obtain detailed information on the pressure evolution of structural parameters. As an example, we show in Fig. 3 the result of the refinement for the pattern collected at 10.3 GPa. The convergence was achieved with a subtracted background at $R_{wp}=0.8\%$, $R_p=0.5\%$, and $R(F^2)=9.0\%$. Corresponding structural parameters are given in Table I.

The pressure dependence of interatomic distances in the scheelite phase is illustrated in Fig. 4. In this structure, each

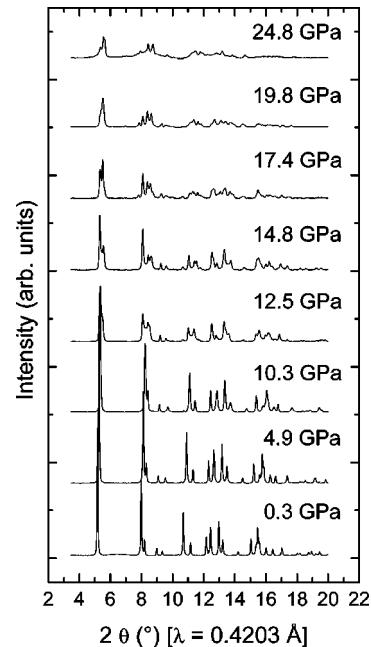


FIG. 2. X-ray powder diffraction patterns of YLiF_4 upon compression without prior annealing of the sample. A smooth background arising mainly from Compton scattering in the diamond anvils is subtracted from all diagrams.

of the cations is surrounded by four near-neighbor cations of the same kind and eight near-neighbor cations of the other kind. All these cation-cation distances would be exactly equal for a c/a axial ratio of two, i.e., for cations in the ideal fluorite arrangement. Such an arrangement would be favored by the electrostatic cation-cation repulsive interactions. On the other hand, the packing of the atoms forces the axial ratio to be greater than two, i.e., it induces a tetragonal distortion of the fluorite structure.^{11,12} It is evident in Fig. 4 that there is no anomaly in the pressure dependence of the intercationic

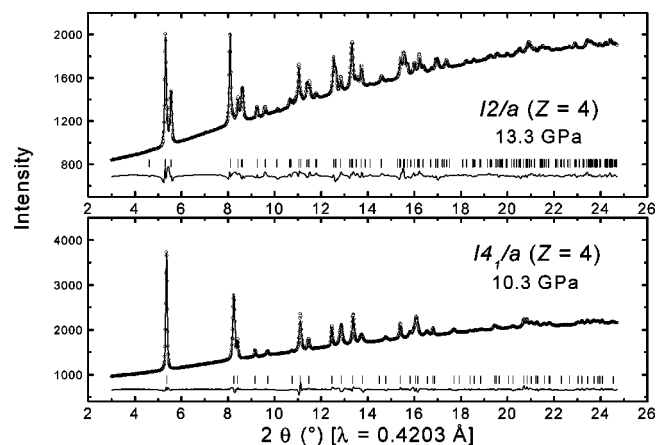


FIG. 3. Observed, calculated, and difference x-ray powder patterns for the scheelite ($I4_1/a$, $Z=4$) and fergusonite ($I2/a$, $Z=4$) phases of YLiF_4 at 10.3 GPa (bottom) and 13.3 GPa (top), respectively. Vertical markers indicate Bragg reflections. The pattern of the fergusonite phase was obtained after precompressing the sample to 17.0 GPa and annealing at 423 K for 3 h.

TABLE I. Structural parameters obtained from a full Rietveld refinement of the diffraction diagram for YLiF_4 collected at 10.3 GPa. The space group is $I4_1/a$ ($Z=4$) the lattice parameters are $a=4.9589(1)$ Å, $c=10.5050(5)$ Å, and the unit cell volume is $V=258.33(2)$ Å³. Positional parameters are given in the upper part, interatomic distances in the bottom part. All distances are in Å. Estimated standard deviations are given in brackets.

Atom	Site	x	y	z
Y	4b	0	1/4	5/8
Li	4a	0	1/4	1/8
F	16f	0.2206(4)	0.5813(8)	0.5400(4)

Atoms	No.	Distance	Atoms	No.	Distance
Y-Li'	4	3.61178(9)	Li-F'	4	1.848(3)
Y-Li''	4	3.50647(9)	Li-F''	4	2.761(4)
Y-F'	4	2.166(4)	F-F	6	2.478(5)
Y-F''	4	2.214(4)	Y-Y	4	3.61178(9)

distances, while the difference between the Y-Li' and Y-Li'' distances increases with pressure. In addition, the c/a axial ratio in this structure also increases, demonstrating that the tetragonal distortion of the fluorite structure is being enhanced (Fig. 5).

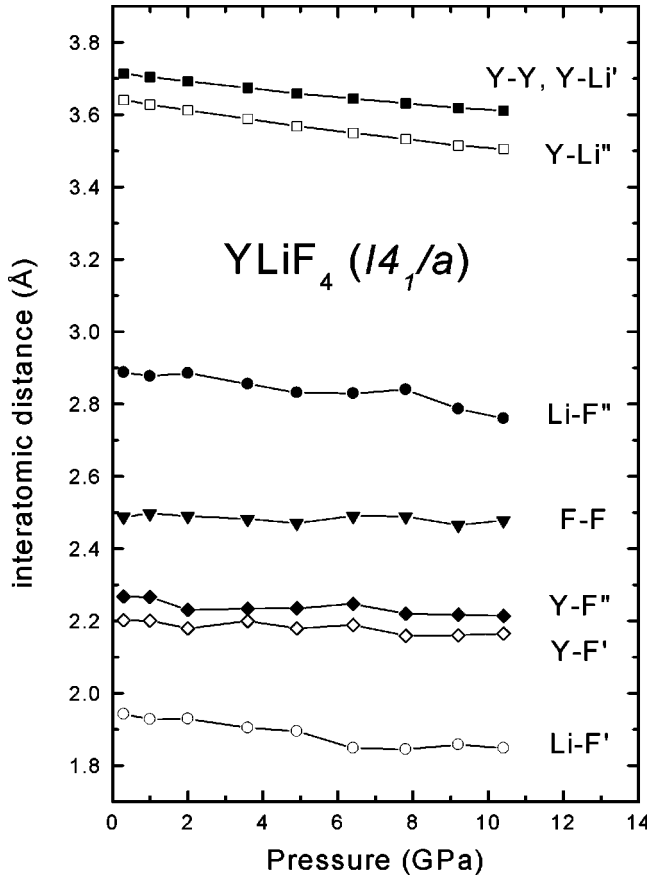


FIG. 4. Pressure dependence of interatomic distances in scheelite YLiF_4 ($I4_1/a$, $Z=4$) up to 10.3 GPa. Representative estimated standard deviations are given in Table I. Lines are guide to the eye.

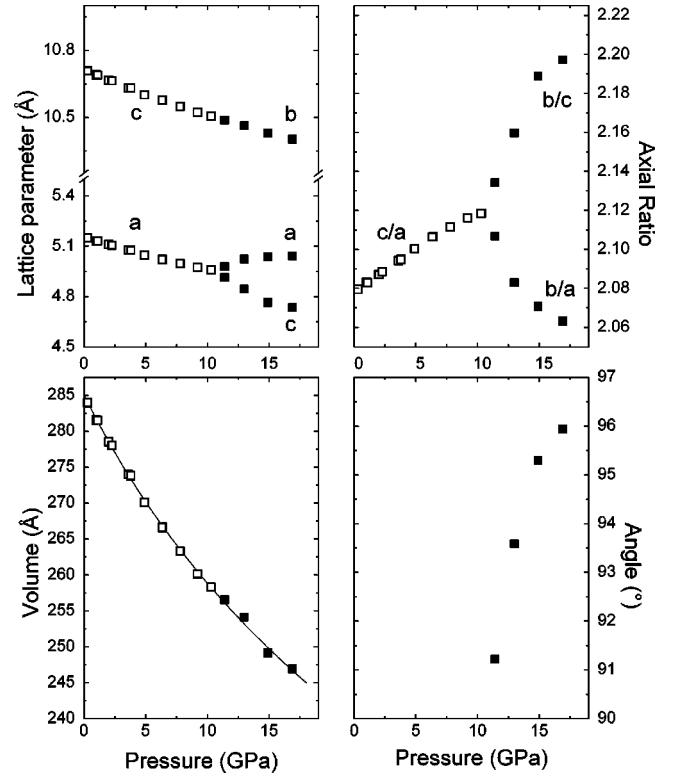


FIG. 5. Pressure dependence of lattice parameters for the scheelite ($I4_1/a$, $Z=4$) and fergusonite ($I2/a$, $Z=4$) phases of YLiF_4 (open and solid symbols, respectively) up to 17.4 GPa.

To determine the structure of the high-pressure phase occurring above 10.3 GPa we used a pattern of the sample pre-compressed to 17.0 GPa and annealed at 423 K for 3 h. After quenching the sample to room temperature, the measured pressure was 13.3 GPa. Such a procedure dramatically improved the quality of the diffraction diagram (see diagram in Fig. 3). The pattern can be indexed¹³ on the basis of an I centered monoclinic unit cell with $a=5.050(2)$ Å, $b=10.437(3)$ Å, $c=4.788(2)$ Å, and $\beta=95.26(4)^\circ$ [indexing figures of merit $M(20)=19.3$ and $F(20)=73.1$]. The volume of 251.25 Å³ suggests that the Z parameter is equal to 4. A peak splitting and appearance of weak reflections at the phase transition (Fig. 2), together with the values of the lattice parameters, imply that this new structure, related to scheelite, is of the fergusonite type ($I2/a$, $Z=4$). It is found, for instance, in rare earth orthoniobates and orthotantalates.¹⁴ Indeed, application of direct methods¹⁵ to solve this structure yields the Y, Li, and F atomic positions [$R(F^2)=15.1\%$ with no Rietveld refinement] that can approximately be derived on the basis of the $I4_1/a \rightarrow I2/a$ subgroup relationship.

The full Rietveld refinement of the profile at 13.3 GPa with the fergusonite model, obtained with direct methods, is shown in Fig. 3. The convergence was achieved with a subtracted background at $R_{wp}=2.0\%$, $R_p=1.2\%$, and $R(F^2)=12.3\%$. The corresponding structural parameters are given in Table II. In the high-pressure fergusonite structure of YLiF_4 , which is a monoclinic superstructure of fluorite, none of the Y-Li intercationic distances is equal to the Y-Y ones. The Li-F bonds and next near-neighbor Li-F distances are

TABLE II. Structural data obtained from a full Rietveld refinement of the pattern for YLiF₄ collected at 13.3 GPa – *I*2/*a* (*Z* = 4), *a* = 5.0416(3) Å, *b* = 10.4174(9) Å, *c* = 4.7808(4) Å, β = 95.279(6)°, *V* = 250.03(3) Å³. Positional parameters are given in the upper part, interatomic distances in the bottom part. All distances are in Å. Estimated standard deviations are given in brackets.

Atom	Site	<i>x</i>	<i>y</i>	<i>z</i>
Y	4 <i>e</i>	1/4	0.8790(3)	0
Li	4 <i>e</i>	1/4	0.362(4)	0
F(1)	8 <i>f</i>	0.430(2)	0.0317(7)	0.756(1)
F(2)	8 <i>f</i>	0.937(1)	0.2962(7)	0.136(2)

Atoms	No.	Distance	Atoms	No.	Distance
Y-Y	4	3.566(4)	Li-F(1)	2	2.76(3)
Y-Li	2	3.55(3)		2	1.83(2)
	2	3.315(2)	Li-F(2)	2	1.89(2)
	2	3.634(2)		2	2.78(2)
	2	3.61(3)	F(1)-F(1)		2.47(1)
Y-F(1)	2	2.216(8)	F(1)-F(2)		2.52(1)
	2	2.120(8)	F(2)-F(2)	2	2.577(6)
Y-F(2)	2	2.128(8)			2.46(2)
	2	2.229(9)			2.19(1)
	2	3.22(1)			

1.83–1.89 Å and 2.76–2.78 Å. Hence, the LiF₄³⁻ tetrahedra are still isolated but largely deformed. In fact, the fergusonite structure of YLiF₄ at high pressures is a distorted and compressed version of the scheelite type (Fig. 1) obtained by a small distortion of the cation matrix and significant displacements of anions,² in a fashion similar to the atomic displacement scheme in rare earth orthoniobates and orthotantalates.¹⁴

We note that the nonstandard setting of space group No. 15 (*I*2/*a*, *Z*=4) is used here because in that way the scheelite and fergusonite structures can easily be compared. The lattice parameters given in Table II become *a* = 6.6211 Å, *b* = 10.4174 Å, *c* = 5.0416 Å, β = 134.028°, and *V* = 250.03 Å³, respectively, in the standard *C*2/*c* setting.

The pressure dependence of the *I*2/*a* lattice parameters is plotted up to 17.4 GPa in Fig. 5. During the scheelite-fergusonite phase transition, there is no discontinuity in the evolution of the unit cell volumes and the *c* tetragonal and *b* monoclinic lattice parameters. It indicates that the volume difference between the two polymorphs either is negligible or is below the detection limit of our x-ray powder diffraction experiment. The β angle, that along with the difference between the *b*/*a* and *b*/*c* axial ratios is the measure of the monoclinic distortion, increases with pressure. It back-extrapolates to 90° at about 10.6 GPa.

The combined compression data for the scheelite and fergusonite polymorphs up to 17.4 GPa have been fitted by a Birch-Murnaghan equation of state (solid line in Fig. 5), giving the zero-pressure bulk modulus $B_0 = 81 \pm 4$ GPa, the first pressure derivative of the bulk modulus $B' = 4.97 \pm 0.68$, and the unit cell volume of scheelite at ambient pres-

sure $V_0 = 285.1 \pm 0.5$ Å³. Our value of B_0 essentially agrees, within experimental uncertainty, with the result derived from ultrasonic experiments ($B_0 = 80$ GPa, Ref. 16).

Unfortunately, our x-ray powder data for the second high-pressure phase observed above 17 GPa do not allow for a reliable structure solution. Prolonged annealing of the sample at high pressures and moderate temperatures (450 K) did not improve the x-ray patterns. Therefore, the structure of the second high-pressure polymorph of YLiF₄ has yet to be determined.

IV. DISCUSSION

The observation of the phase transition of YLiF₄ at 10.6 GPa is in accord with luminescence experiments on YLiF₄:Eu at *T* = 300 K which evidenced a reversible, possibly continuous, transformation in the pressure range from 10.0 to 10.5 GPa, due to lowering of the crystal symmetry.⁵ The low-temperature luminescence study of crystal field transitions in YLiF₄:Nd also indicated a phase transition near 10 GPa, which, however, showed pronounced hysteresis effects.⁶ The very subtle changes in pressure coefficients of luminescence band energies near 6 GPa reported in the latter study possibly have a structural origin, but the details are not resolved of the present experiments. The rather abrupt change in the pressure dependence of internal vibrational LiF₄³⁻ modes at 7.0 GPa seen in the Raman spectra of YLiF₄ (Ref. 4) cannot be understood on the basis of our structural data. It remains to be seen whether the phase transition at 7 GPa indicated by the Raman data was possibly driven by nonhydrostatic conditions or is due to the fact that the results were obtained for undoped YLiF₄.

The transition to the fergusonite structure (*I*2/*a*, *Z*=4) involves small distortions of the cation matrix and significant displacements of anions away from a simple cubic packing. Both scheelite and fergusonite polymorphs are superstructures of the fluorite type (*Fm* $\bar{3}$ *m*, *Z*=2). There is no discontinuity in the evolution of the unit cell volumes during the *I*4₁/*a* → *I*2/*a* structural change.

The observed changes of the *a* and *c* lattice parameters as well as *b*/*c* and *b*/*a* ratios are strikingly similar to those found for temperature-induced¹⁷ (or negative pressure-induced¹⁸) scheelite-fergusonite transitions in rare earth orthoniobates and orthotantalates. The temperature-induced transitions are ferroelastic with the order parameter being an elastic strain.^{14,17} Several efforts have been made to understand the mechanism of this transformation, but it still remains uncertain whether it is of the first or second order.^{17,19} Associated with the transformation is the anisotropic phonon softening of a transverse acoustic mode at the Brillouin zone center. Our x-ray powder diffraction data on YLiF₄ at high pressures, e.g., the evolution of the lattice parameters, do not provide any direct evidence for a pressure-induced ferroelastic phase transition in this material. In this context we note, however, that Blanchfield *et al.*¹⁶ investigated the elastic behavior of fluoroscheelites under pressure and observed a softening of near-zone-center acoustic modes in these crystals.

To the best of our knowledge, the new high-pressure poly-

morph of YLiF_4 is the first reported fergusonite phase in orthohalides. Lanthanide tetrafluorides of sodium and potassium are also derivatives of the fluorite type; however, the ideal cubic structure is present in LnNaF_4 ($\text{Ln} = \text{Ho-Lu, Y}$) (Ref. 20) and LnKF_4 ($\text{Ln} = \text{La, Ce}$) (Ref. 21) while the compounds LnKF_4 ($\text{Ln} = \text{Gd-Lu, Y}$) (Ref. 22) have a trigonal superstructure ($P3_1, Z=18$). CeKF_4 is dimorphous with cubic ($Fm\bar{3}m, Z=2$) and orthorhombic ($Pnma, Z=4$) phases.²³ The structural systematics in corresponding tetrachlorides is more complicated. GdLiCl_4 has the scheelite structure.²⁴ At low temperatures, a triclinic lattice ($P\bar{1}, Z=2$) of the LnNaCl_4 compounds ($\text{Ln} = \text{Eu-Yb, Y}$) is derived from the fluorite type.^{25,26} Their high-temperature structure is of the wolframite (Fe,MnWO_4 type ($P2/c, Z=2$), that is a superstructure of rutile TiO_2 ($P4_2/mnm, Z=2$), in which the metal atoms occupy one-quarter of the octahedral sites in a distorted hexagonal close packing (*hcp*) of the anions. ScNaCl_4 and LuNaCl_4 are orthorhombic ($Pbcn, Z=4$) and related to wolframite.^{27,28}

All structural relationships both in the fluorides and chlorides and the change from the simple cubic to hexagonal close packing of the anions could be explained on the basis of ionic radii, similar to the high-pressure structural systematics in ABO_4 ternary oxides.^{29,30} Some known high-pressure phases may illustrate general trends and lead to possible structure candidates for the second high-pressure phase of YLiF_4 . The scheelite structure is the high-pressure form of the zircon ZrSiO_4 ($I4_1/amd, Z=4$), monazite CePO_4 ($P2_1/n, Z=4$), and CrVO_4 ($Cmcm, Z=4$) types. Pressure-induced transformations scheelite-wolframite have been proposed for molybdates and tungstates.³¹ Another possible transition in scheelite-structured materials is to the $\text{BaWO}_4(\text{II})$ type ($P2_1/n, Z=8$). The rare earth orthoniobate and orthotantalate fergusonites transform to the LaTaO_4 ($P2_1/c, Z=4$) or BaMnF_4 ($Cmcm, Z=4$) types.³² In all

these post-scheelite (post-fergusonite) structures, the coordination of the *B* cation is higher than four while the anions are in a distorted hexagonal close packing. It should be recalled that the wolframite related structures already occur for some orthochlorides at ambient pressure: LnNaCl_4 ($\text{Ln}=\text{Eu-Yb, Y}$) in space group $P2/c$ ($Z=2$)(8,9), and ScNaCl_4 and LuNaCl_4 in space group $Pbcn$ ($Z=4$).^{27,28} Based on these considerations, it cannot be ruled out that the second high-pressure polymorph of YLiF_4 occurring above about 17.0 GPa has a hexagonal close packed arrangement of the anions.

V. CONCLUSIONS

The present structural study of YLiF_4 provides quantitative information on pressure-induced changes of the cation coordinations in the scheelite phase. These results are considered important for modelling the pressure-dependence of crystal field levels of lanthanide ions introduced in this laser host material. The scheelite phase of YLiF_4 is found to undergo a structural phase transition near 10 GPa. The high-pressure phase has the fergusonite structure. The structural details of the scheelite-fergusonite transition in YLiF_4 show striking similarities to temperature-driven scheelite-fergusonite transitions in rare earth orthoniobates and orthotantalates. Our observations warrant further studies to elucidate this transformation of YLiF_4 and examine the possibility of the soft acoustic phonon involved in it. We have observed a second high-pressure phase transition of YLiF_4 , starting at 17 GPa. The structure of this phase remains to be solved.

ACKNOWLEDGMENTS

The authors acknowledge stimulating discussions with F. J. Manjon and S. Jandl. We thank U. Oelke for technical assistance during the experiments.

*Corresponding author; Email address: andrzej@servix.mpi-stuttgart.mpg.de.

¹R.E. Thoma, G.D. Brunton, R.A. Penneman, and T.K. Keenan, *Inorg. Chem.* **9**, 1096 (1970).

²A.V. Goryunov, A.I. Popov, and N.M. Khajdukov, *Mater. Res. Bull.* **27**, 213 (1992); E. Garcia and R.R. Ryan, *Acta Crystallogr., Sect. C: Cryst. Struct. Commun.* **49**, 2053 (1993).

³B. Bihari, K.K. Sharma, and L.E. Erickson, *J. Phys.: Condens. Matter* **2**, 5703 (1990); S. Salaün, M.T. Fornoni, A. Bulou, M. Rousseau, P. Simon, and J.Y. Gesland, *ibid.* **9**, 6941 (1997); S. Salaün, A. Bulou, M. Rousseau, B. Hennion, and J.Y. Gesland, *ibid.* **9**, 6957 (1997); A. Sen, S. L. Chaplot, and R. Mittal, *Phys. Rev. B* **64**, 024304 (2001). See also literature cited in these references.

⁴E. Sarantopoulou, Y.S. Raptis, E. Zouboulis, and C. Raptis, *Phys. Rev. B* **59**, 4154 (1999).

⁵L. Shenxin, C. Yuanbin, Z. Xuyi, and W. Lizhong, *J. Alloys Compd.* **255**, 1 (1997).

⁶J. F. Manjon, S. Jandl, K. Syassen, and J. Y. Gesland, *Phys. Rev. B* **64**, 235108 (2002).

⁷A.P. Hammersley, S.O. Svensson, M. Hanfland, A.N. Fitch, and

D. Häusermann, *High Press. Res.* **14**, 235 (1996).

⁸G. J. Piermarini, S. Block, J. D. Barnett, and R. A. Forman, *J. Appl. Phys.* **46**, 2774 (1975); H. K. Mao, J. Xu, and P. M. Bell, *J. Geophys. Res.* **91**, 4673 (1986).

⁹A. C. Larson and R. B. von Dreele, *GSAS: General Structure Analysis System*, Los Alamos National Laboratory, 2000.

¹⁰P. W. Stephens, *J. Appl. Crystallogr.* **32**, 281 (1999).

¹¹B.G. Hyde and S. Andersson, *Inorganic Crystal Structures* (Wiley, New York, 1989).

¹²O. Muller and R. Roy, *The Major Ternary Structural Families* (Springer-Verlag, Berlin, 1974), p. 83.

¹³A. Boultif and D. Louer, *J. Appl. Crystallogr.* **24**, 987 (1991).

¹⁴S. Tsunekawa, T. Kamiyama, K. Sasaki, H. Asano, and F. Fukuda, *Acta Crystallogr., Sect. A: Found. Crystallogr.* **49**, 595 (1993); S. Tsunekawa, T. Kamiyama, H. Asano, and T. Fukuda, *J. Solid State Chem.* **116**, 28 (1995); S.V. Borisov and E.N. Ipatova, *J. Struct. Chem.* **35**, 865 (1994).

¹⁵A. Altomare, M.C. Burla, M. Camalli, B. Carrozzini, G.L. Cascarano, C. Giacovazzo, A. Guagliardi, A.G.G. Moliterni, G. Polidori, and R. Rizzi, *J. Appl. Crystallogr.* **32**, 339 (1999).

¹⁶P. Blanchfield, G. A. Saunders, and Tu Hailing, *J. Phys. C* **15**, 2081 (1982).

- ¹⁷I.A. Kondrat'eva, S.K. Filatov, L.V. Andrianova, and A.M. Korovkin, *Inorg. Mater. (Transl. of Neorg. Mater.)* **25**, 1446 (1989); K. Parlinski, Y. Hashi, S. Tsunekawa, and Y. Kawazoe, *J. Mater. Res.* **12**, 2428 (1997).
- ¹⁸J.W.E. Mariathasan, L.W. Finger, and R.M. Hazen, *Acta Crystallogr., Sect. B: Struct. Sci.* **41**, 179 (1985).
- ¹⁹Y. Kuroiwa, H. Muramoto, T. Shobu, H. Tokumichi, Y. Noda, and Y. Yamada, *J. Phys. Soc. Jpn.* **64**, 3798 (1995); Y. Kuroiwa, K. Nozawa, J. Ikegami, T. Shobu, Y. Noda, and S. Tsunekawa, *J. Korean Phys. Soc.* **32**, S84 (1998); Y. Kuroiwa, S. Aoyagi, T. Shobu, K. Nozawa, S. Tsunekawa, and Y. Noda, *Jpn. J. Appl. Phys.* **38**, 600 (1999).
- ²⁰D.M. Roy and R. Roy, *J. Electrochem. Soc.* **111**, 421 (1964).
- ²¹W.H. Zachariasen, *Acta Crystallogr.* **2**, 388 (1949).
- ²²Y. Le Fur, N.M. Khaidukov, and S. Aleonard, *Acta Crystallogr., Sect. C: Cryst. Struct. Commun.* **48**, 978 (1992).
- ²³G. Brunton, *Acta Crystallogr.* **25**, 600 (1969).
- ²⁴G. Meyer, *Z. Anorg. Allg. Chem.* **511**, 193 (1984).
- ²⁵T. Schleid and G. Meyer, *Z. Anorg. Allg. Chem.* **590**, 103 (1990).
- ²⁶M.S. Wickleder and G. Meyer, *Z. Anorg. Allg. Chem.* **621**, 546 (1995).
- ²⁷A. Bohnsack, G. Meyer, and M. Wickleder, *Z. Kristallogr.* **211**, 394 (1996).
- ²⁸M.S. Wickleder, H.U. Guedel, T. Armbruster, and G. Meyer, *Z. Anorg. Allg. Chem.* **622**, 785 (1996).
- ²⁹O. Fukunaga and S. Yamaoka, *Phys. Chem. Miner.* **5**, 167 (1979).
- ³⁰R.M. Hazen, L.W. Finger, and J.W.E. Mariathasan, *J. Phys. Chem. Solids* **46**, 253 (1985).
- ³¹D. Christofilos, G.A. Kourouklis, and S. Ves, *J. Phys. Chem. Solids* **56**, 1125 (1995); S.R. Shieh, L.C. Ming, and A. Jayaraman, *ibid.* **57**, 205 (1996).
- ³²Y. Titov, A.M. Sych, A.N. Sokolov, A.A. Kapshuk, and V.P. Yashchuk, *Inorg. Mater. (Transl. of Neorg. Mater.)* **33**, 60 (1997); Y.A. Titov, A.M. Sych, A.N. Sokolov, A.A. Kapshuk, and V.P. Yashchuk, *ibid.* **36**, 625 (2000); Y.A. Titov, A.M. Sych, A.N. Sokolov, A.A. Kapshuk, V.Y. Markiv, and N.M. Belyavina, *J. Alloys Compnd.* **311**, 252 (2000).